 DOI: 10.1002/masy.201050524

Physical Gels Based on Polyrotaxanes: Kinetics of the Gelation, and Relative Contributions of α-Cyclodextrin and Poly(ethylene oxide) to the Gel Cohesion

Christophe Travelet,[1] *Guy Schlatter,*[*1] *Pascal Hébraud,*[2] *Cyril Brochon,*[1] *Denis V. Anokhin,*[3] *Dimitri A. Ivanov,*[3] *Georges Hadziioannou*[1]

Summary: Polyrotaxanes (PRs) based on α-cyclodextrins (α-CDs) threaded onto 22 kg mol^{-1} poly(ethylene oxide) (PEO) chains in concentrated solution in dimethyl sulfoxide (DMSO) showed the particularity to form physical gels when resting at 21 °C. The wide range of studied degrees of complexation *N* (from 7 up to 176), where *N* is the number of threaded α-CDs per PEO chain, allowed to better understand the molecular origin of the physical gelation. The non-monotonous evolution of the mechanical properties of the gels with the complexation degree can be attributed to the crystallization of naked PEO segments and the aggregation of α-CDs. In fact, differential scanning calorimetry measurements carried out on these physical gels showed two distinct endothermic peaks. The first peak at 29.4 °C was attributed to the crystals of naked PEO segments (the parts of the PR molecule not covered by α-CDs). The second peak at 32.0 °C was attributed to α-CD aggregates. The dissolution enthalpy of the low temperature peak decreased monotonously with increasing *N* and the dissolution enthalpy of the high temperature peak increased monotonously with increasing *N*. These results were confirmed using X-ray scattering and ^{1}H NMR spectroscopy measurements showing these two contributions to gelation. These results showed that the cohesion of the physical gel was due to the crystallization of naked PEO segments, on the one hand, and, on the other hand, to the regular aggregation of α-CDs driven by intra- and inter-molecular hydrogen bonding interactions of their hydroxyl groups.

Keywords: association; crystallization; gels; polyrotaxanes; supramolecular structures

Introduction

Polyrotaxane (PR) is a pearl necklace shape supramolecule in which many macrocycles are threaded onto a single guest polymer chain whose ends are capped with bulky groups to prevent dethreading.[1] Among them, PRs formed with α–cyclodextrins (α–CDs) as macrocycles have been widely studied.[1] α–CDs are composed by the repetition of six glucose units organized in a truncated conical form. Among the eighteen hydroxyl groups carried by an α–CD, twelve of them point outside the molecule, whereas the remaining six are directed towards the inner cavity. Favorable hydrophobic interactions between the inner cavity of the α–CDs and guest polymer chains such as poly(ethylene oxide) (PEO) can be tuned by choosing, for instance, an appropriate temperature[2] or an adequate

[1] Laboratoire d'Ingénierie des Polymères pour les Hautes Technologies, Ecole Européenne de Chimie, Polymères et Matériaux, Université Louis Pasteur de Strasbourg, CNRS UMR 7165, 25 rue Becquerel, 67087 Strasbourg Cedex 2, France
Fax: +33 (0)3 90 24 27 16;
E-mail: Guy.Schlatter@ecpm.u-strasbg.fr
[2] Institut de Physique et Chimie des Matériaux de Strasbourg, CNRS UMR 7504, Université Louis Pasteur de Strasbourg, 23 rue du Loess, BP 43, 67034 Strasbourg Cedex 2, France
[3] Institut de Chimie des Surfaces et Interfaces, CNRS UPR 9069, 15 rue Jean Starcky, BP 2488, 68057 Mulhouse Cedex, France

composition of the solvent mixture.[3] Thus, PEO threads into the α–CDs in a controlled way, forming PRs characterized by a given number of threaded α–CDs per PEO chain, which can be varied over a wide range.

In the present study, we show that PRs based on α–CD and PEO in concentrated DMSO solution form a physical gel with time at room temperature. Moreover, we precisely identify the interactions responsible for the physical gelation of PRs. For this, we studied PRs based on α–CD and PEO with a molecular weight of 22 kg mol^{-1} and various complexation degrees *N*, *i.e.* different numbers of threaded α–CDs per PEO chain, ranging from 7 up to 176. From complementary experimental techniques, the origin of the physical gelation of the PR solutions was elucidated. We demonstrated that two distinct contributions led to the formation of physical gels: (a) the crystallization of naked PEO segments, i.e. the ethylene oxide units of the PEO chains not covered by α–CDs, and, (b) the aggregation of α–CDs due to intra– and inter–molecular hydrogen bonding.

Experimental Part

Materials and Polyrotaxane Synthesis

Dihydroxy-terminated PEO was purchased from Serva Electrophoresis® and dried by azeotropic distillation from toluene before use. A number-average molecular weight of 22 kg mol^{-1} and a polydispersity index of 1.03 were measured using gel permeation chromatography (GPC) in DMSO at 70 °C and a molecular weight calibration constructed using PEO standards. DMSO (from Riedel–de Haën®) was distilled over potassium hydroxide under reduced pressure. Deuterated dimethyl sulfoxide with 99.9% enrichment (DMSO-d_6) (from Aldrich®) was used as received without any further purification.

PRs based on α–CDs as macrocycles, α,ω–bis–amine–terminated PEO (synthesized from dihydroxy-terminated PEO according to an adaptation of the procedure of Mutter[4]) as guest chains and 2,4–dinitro–1–fluorobenzene as bulky groups were synthesized according to an adaptation of the procedure of Fleury.[2] The PRs were obtained at yields between 3 and 24% mol relative to the α,ω-bis-amine-terminated PEO. The values of the complexation degree were estimated using ^{1}H NMR spectroscopy in DMSO-d_6, whereas the efficiency of the capping step was determined using GPC in HPLC grade DMSO at 70 °C.[2]

Characterization Methods

Nuclear Magnetic Resonance

(^{1}H NMR) spectra were recorded on a spectrometer from Bruker® and operating at a frequency of 400 MHz with 24 scans per spectrum. Each spectrum of a non-spinning sample required approximately 2.5 min to be measured. The PR solutions in DMSO-d_6 were introduced in the NMR tubes and heated up at 43 °C in a water bath during 5 min. Then, the tubes were rapidly introduced in the spectrometer pre-cooled at 21.0 ± 0.5 °C and spectra were continuously recorded during 100 min. The internal lock was made on the ^{2}H-signal of the solvent.

Rheological Dynamic Analysis

(RDA) was performed on the Physica MCR 301 rheometer commercialized by Anton Paar® and equipped with the P-PTD 200 + H-PTD 200 Peltier system allowing heating or cooling in the range of −40 to 200 °C. The rheometer could be strain controlled via a control loop or stress-controlled. The used configuration was the CP 25-2 cone-plate geometry supplied by Anton Paar® with a cone angle of 2°, a diameter of 25 mm and a cone truncation of 49 μm. In order to achieve an initial state as reproducible as possible, the PR solutions in DMSO were heated up at 43.0 ± 0.1 °C while being continuously sheared at a shear rate of 40 s^{-1}. After 10 min under these conditions, the solutions were cooled down at 21.0 ± 0.1 °C. When this temperature was reached, the elastic modulus (G′) and the loss modulus (G″) were continuously recorded during a few hours at an angular

frequency of $1\,rad\,s^{-1}$. Due to the large variation of the mechanical response of the mixtures with time, the following procedure was automated: At the beginning of the measurement, while the system was fluid enough, a constant stress of 0.1 Pa was applied. Then, as soon as the resulting deflection angle fell below the rheometer resolution, *i.e.* 7.0×10^{-5} rad, a constant strain of 0.3% was imposed.

Differential Scanning Calorimetry

(DSC) thermograms were recorded on the DSC 2910 calorimeter commercialized by TA Instruments® and equipped with a liquid nitrogen cooling accessory allowing continuous programmed cooling in the range of −150 to 725 °C. The pressure DSC cells supplied by TA Instruments® were filled in with the PR solutions in DMSO. Afterwards, they were heated up to 43 °C and immediately cooled down at 21 °C at a heating/cooling rate of +/− 5.0 ± 0.1 °C min^{-1}. Then, the cells were kept at 21.0 ± 0.1 °C inside the DSC apparatus during a given aging time t_a varying between 1 min and 52 h and finally heated up to 43 °C at a heat rate of 5.0 ± 0.1 °C min^{-1}. A supplementary measurement point at $t_a = 16$ days (384 h) was obtained after keeping the cells in a room at 21 ± 2 °C.

Wide Angle X-ray Scattering

(WAXS) measurements were made on the BM26 and ID02 beamlines at the European Synchrotron Radiation Facility (ESRF, Grenoble, France). The energies of X-ray photons were 10 keV for BM26 and 12 keV for ID02, which corresponded to wavelengths of 0.12 nm and 0.10 nm, respectively. The modulus of the scattering vector ($q = 4\pi \sin(\theta/2)/\lambda$) was calibrated using several diffraction orders of silver behenate. The solutions were first heated up at 43 °C. Then, they were cooled down at 21 °C. The samples were measured after a long aging time (typically 24 h) at this temperature. The total volume crystallinity at a given time was defined as the ratio of intensity of all crystalline peaks over the total intensity corrected by the background and the Lorentz factor. The volume crystalline ratios are given with respect to the whole PR system volume.

Results and Discussion

PRs with well-defined *N*-values (*i.e.* the number of threaded α-CDs per PEO chain), ranging from 7 to 176, were obtained thanks to the methodology previously reported.[2] In the following, the PRs will be denoted PR_N, where the subscript *N* indicates the complexation degree *N*. Since PEO with a molecular weight of $22\,kg\,mol^{-1}$ was used, the α-CD overlap ratio (*i.e.* the percentage of ethylene oxide units of the PEO chains which could be covered by α-CDs) ranged from 3 to 70%. A concentrated PR solution in DMSO heated up at 43 °C was fluid. When cooled down at 21 °C, it gelled slowly with time. This process was fully thermo-reversible as the formed gel returned to its original fluid state and remained fluid when heated up at 43 °C. Thus, we chose to follow the evolution with time of the mechanical properties of the PR solutions when quenched from 43 °C down to 21 °C, *i.e.* 3 °C above the crystallization temperature of pure DMSO.

Macroscopic Signature of Gelation

RDA measurements were performed on PR_7, PR_{37}, PR_{85} and PR_{157} concentrated solutions (19.6 w/w%) in DMSO. The typical evolution of the elastic (G′) and the loss (G″) moduli at an angular frequency of $1\,rad\,s^{-1}$ with time at 21 °C in the case of PR_7 is given in Figure 1a. Three distinct time domains were observed: At first, the system was liquid, the elastic modulus G'_0 was lower than the loss modulus and both remained constant with time during a so-called induction time. Afterwards, the two moduli crossed-over each other and increased strongly. Finally, the elastic modulus became one order of magnitude higher than the loss modulus, and, subsequently, both moduli evolved slowly with time to an asymptotic value

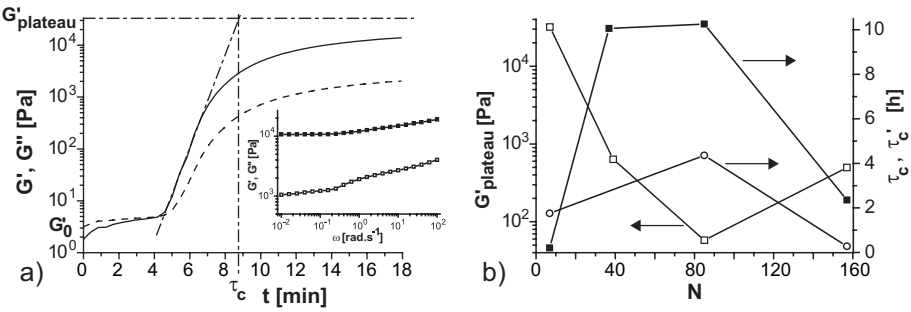

Figure 1.

RDA: a) (solid line) Elastic modulus G′ and (dashed line) loss modulus G″ at an angular frequency of 1 rad s^{-1} *versus* time *t* at 21 °C for PR_7 at 19.6 w/w% in DMSO. G'_0 is the value of the elastic modulus at an angular frequency of 1 rad s^{-1} at short times and $G'_{plateau}$ its value at long times. Inset: (■) elastic modulus G′ and (□) loss modulus G″ *versus* angular frequency ω for PR_7 at 19.6 w/w% in DMSO after 18 min at 21 °C. b) (□) Elastic modulus $G'_{plateau}$ at long times at an angular frequency of 1 rad s^{-1}, (■) characteristic time τ_c determined through RDA measurements and (○) characteristic time τ_c' determined through DSC measurements *versus* complexation degree *N* for PRs at 19.6 w/w% in DMSO at 21 °C.

($G'_{plateau}$ as far as the elastic modulus is concerned). In the last regime, the elastic modulus no longer depended on the angular frequency between 10^{-2} and 10^{2} rad s^{-1} (inset of Figure 1a): A physical gel was formed.

Different mechanisms can be proposed for the existence of the observed induction time:

– It may correspond to the time necessary for physical cross-link points to self-organize in a 3D percolated structure. Links may be formed prior to the global gelation of the solution and play the role of nucleation points. In the general case, these pre-gel structures could constitute weakly branched polymer chains, clusters[5,6] or nucleation sites.[7] Theoretical studies also reported that a thermoreversible behavior was due to weak junctions between associating groups or segments in an intra- and/or inter-molecular way. These junctions could have various functionalities.[8–10] In our case, these structures consisted of both α-CD clusters and PEO nucleation sites. When the percolation step was achieved, the viscoelastic moduli increased abruptly. Usually, the induction time of physical gelation is much longer than the one of chemical gelation due to the possibility of rearrangement of the conformation of the physical links.
– It may also correspond to the time needed to overcome the energy barrier leading to the formation of one cross-link point. Such an induction time is known for physical gelation of sugar derivative polymers such as agarose,[11] konjac glucomannan[12] and methylcellulose[11] having semi-rigid structure. On the contrary, galactomannan[13] and poly(vinyl alcohol)[14] have very flexible coil-type structure and consequently can easily and rapidly change their conformations so as to find the most adequate position for association and gelation to occur. Thus, they do not show any induction time before their physical gelation.[13,14]

PRs in DMSO solution have different structures as a function of the number of threaded α-CDs per PEO chain. Indeed, PR_7 is much more flexible than PRs with higher complexation degrees. These differences may thus be responsible for the very short induction time for PR_7 and the longer ones observed at higher complexation degrees.

Furthermore, the kinetics of evolution of the moduli for the different complexation degrees were compared by considering a characteristic time τ_c. This time was defined

as the intersection point between the tangent at the inflection point and the asymptote at long times of the G' profiles (Figure 1a). The characteristic time τ_c as well as the plateau elastic modulus $G'_{plateau}$ (Figure 1b) were not monotonous functions of the complexation degree. At low complexation degrees N, τ_c increased with the complexation degree. It then decreased at high N values. $G'_{plateau}$ showed the opposite tendencies. The decrease of $G'_{plateau}$ for $N \leq 85$ was attributed to the decrease of the number of cross-linked domains formed by naked PEO segments which were in bad solvent.[15] The increase of $G'_{plateau}$ for $N \geq 85$ was attributed to two origins: the increase of the concentration of α-CD aggregates, on the one hand, and the increase of the PR stiffness, on the other hand, at high N values. Indeed, the α-CD mole number did not increase significantly to explain by itself the strong increase of $G'_{plateau}$. However, it has been demonstrated that with increasing N the stiffness of PR increased significantly.[2]

Thus, two different gelation phenomena occurred. At low N, a large fraction of the PEO chains was not covered by α-CDs, and local precipitation of naked PEO segments formed the physical cross-linked domains of the gel. At high N, α-CD aggregates contributed to the gel cohesion. This implies a phase separation between the aggregated domains (made of α-CDs and naked PEO segments) and the solvent, the non-aggregated PR molecule parts forming the strands of the gel network.

Role of α-Cyclodextrin and Poly(ethylene oxide) in Gelation

To identify the implication of α-CD and PEO functional groups in the gelation, ^{1}H NMR spectroscopy measurements were carried out on PR_{85} at 19.6 w/w% in DMSO-d_6. The signals of diluted PR solutions have already been assigned.[2] The same characteristic peaks were also found, albeit a bit broader, on the performed measurements in the concentrated regime. The signals of all α-CD hydroxyl groups – OH(2), OH(3) and OH(6) (Figure 2c) – were significantly shifted during gelation whereas the signals of the other α-CD functional groups such as the tertiary proton CH(1) were almost not affected (Figure 2a). This suggested the formation of hydrogen bonds between α-CDs and PEO, contributing to gelation. During the gelation process, the electronic environment of the α-CD hydroxyl group OH(3) was a bit less affected than that of the α-CD hydroxyl groups OH(2) and OH(6). On the one hand, the α-CD hydroxyl group OH(2) is directed inside the α-CD cavity (Figure 2c) and could thus only interact in an intramolecular way. The shift of this characteristic peak could not be due to the formation of α-CD tubes resulting from the stacking of few α-CD units along the PEO chain since these were already present in the pre-gel system.[16] From our point of view, the only realistic explanation of this shift was the change of the electronic environment along the α-CD tubes resulting from the modification of the equilibrium distance between adjacent

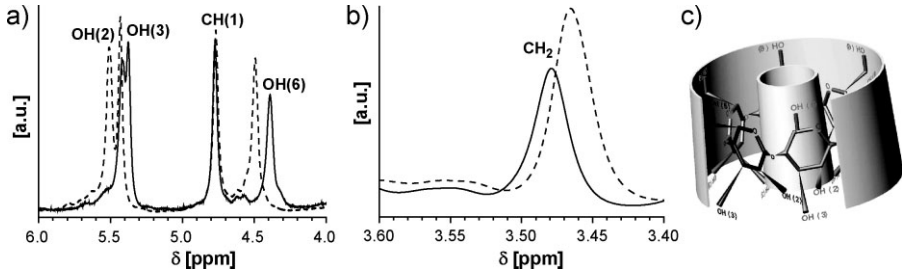

Figure 2.
^{1}H NMR: Spectra showing some characteristic peaks of: a) the α-CD macrocycle of the PR molecule and b) the PEO chain of the PR molecule for PR_{85} at 19.6 w/w% in DMSO-d_6 at $t = 0$ (solid line) and at $t = 100$ min (dashed line) at 21 °C. c) Schematic 3D representation of an α-CD molecule.

stacked α-CDs, *i.e.* belonging to the same tube. On the other hand, the α-CD hydroxyl group OH(3) was directed outside the α-CD cavity and OH(6) is a mobile secondary hydroxyl group (Figure 2c). Both groups could thus be involved in the gelation in an intra- and/or inter-molecular way. The shift of their characteristic peaks was thus responsible for the formation of aggregates resulting from the association of the α-CD tubes as well as in the modification of the equilibrium distance between adjacent stacked α-CDs coming from the formation of aggregates. The signal of the PEO group CH_2 was much less, but still, shifted compared to the α-CD hydroxyl groups (Figure 2b). Indeed, the carbon atoms were located in the external corona of the crystal helix.[17] Consequently, the carbon atoms belonging to neighboring PEO chains faced one another. Thus, the observed upfield shift of the CH_2 peak was consistent with a crystalline state of naked PEO segments. Whereas the chemical shift of CH_2 was weak and should be considered with prudence, this result indicated that naked PEO segments contributed to the gelation of the PR_{85} solution.

During gelation, local α–CD demixing with regard to the naked PEO segments and DMSO was suggested by RDA and ^{1}H NMR spectroscopy. Thus, it was interesting to study if such a demixing led to crystallization. Indeed, Wide Angle X-ray Scattering (WAXS) patterns exhibited two intense quite narrow peaks together with a number of broader much less intense ones (Figure 3a). The positions of the peaks at $q = 13.5\,nm^{-1}$ (corresponding to the Miller indices[17] (hkl) = (120)), $16.5\,nm^{-1}$ ((112), (032) and (13-2)), $18.5\,nm^{-1}$ (024), $19.5\,nm^{-1}$ (22-4) and $25.5\,nm^{-1}$ ((124) and (044)) were not influenced by the complexation degree. They were also found in the pattern of pure PEO at 4.5 w/w% in DMSO and were identical to the conventional monoclinic crystalline phase of PEO. Thus, DMSO being a bad solvent for PEO at 21 °C,[15] crystallization of the naked PEO segments of the PR molecules in DMSO was observed at this temperature. For all studied PR_N and even for the pure PEO, the lateral size of the crystals formed by the naked PEO segments in the (120) direction was estimated with the Scherrer equation[18] to be 27 ± 5 nm. In addition to the PEO peaks, a weak peak at $q = 14.0\,nm^{-1}$ was visible in the patterns at high N values ($N \geq 85$, Figure 3b) whose relative intensity increased with the complexation degree. This could be attributed to the (210) peak of the α–CD crystal structure.[19] This structure could be due to the formation of α–CD tubes originating from attractive intramolecular hydrogen bonding interactions,[20,21] followed by the regular aggregation of these tubes due to attractive intermolecular hydrogen bonding.

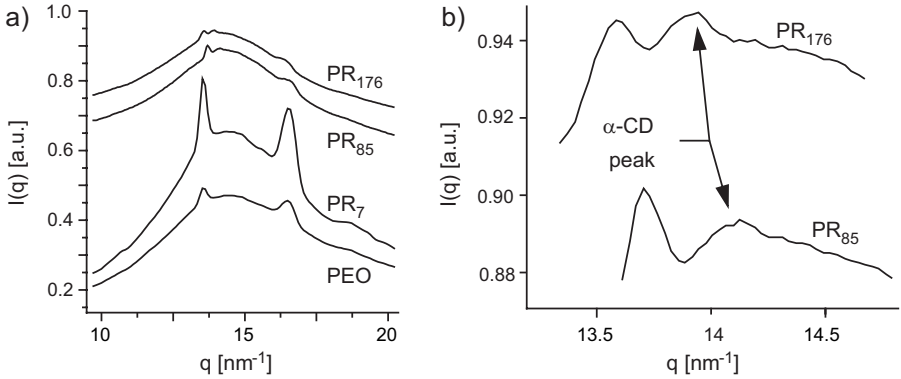

Figure 3.
WAXS intensity *I(q)* versus modulus of the scattering vector *q* for PRs at 19.6 w/w% in DMSO after a long aging time at 21 °C and for PEO at 4.5 w/w% in DMSO after a long aging time at 21 °C.

Thus, for lower N values, the formation of naked PEO segment crystallites was predominant whereas at higher N a second contribution due to well-organized α–CD aggregates participated in gel cohesion.

In order to distinguish between the two contributions and quantify them, we used DSC to follow the association between α-CDs and between naked PEO segments with time at 21 °C.

DSC experiments performed on PR_N, with $N \geq 37$, in solution at 19.6 w/w% in DMSO showed the development of two dissolution peaks with increasing aging time t_a for which the mixture was kept at 21 °C (see the example in Figure 4a for PR_{85}). The temperature position of the peaks, obtained after deconvolution of the mass heat flow curves using two Gaussian functions, was independent of the aging time and of the complexation degree N: 29.4 ± 0.2 °C and 32.0 ± 0.2 °C. In the case of PR_7, DSC thermograms showed monomodal profiles with a peak at 29.4 ± 0.2 °C. Furthermore, DSC measurements carried out on pure PEO at 4.5 w/w% in DMSO revealed a monomodal thermogram with a dissolution peak at 29 ± 0.2 °C. Thus, the low-temperature peak at 29.4 °C was assigned to the dissolution of the PEO crystals whereas the high temperature peak at 32.0 °C corresponded to the dissolution of the organized α–CD aggregates.

The deconvolution of the mass heat flows Q resulted in two dissolution enthalpies ΔH_{PEO} and $\Delta H_{\alpha-CD}$. At long aging time, *i.e.* when gel formation was achieved, a decrease of ΔH_{PEO} and an increase of $\Delta H_{\alpha-CD}$ with N were observed in Figure 4b. When N increased from 7 to 176, the number of naked PEO units and ΔH_{PEO} decreased by the same factor of 22. However, when N increased from 37 to 176, the number of α–CDs increased by a factor of 1.4 whereas $\Delta H_{\alpha-CD}$ increased by a factor of 2.9. These results indicated that α–CDs, contrary to PEO, favored efficiently their own aggregation due to the presence of eighteen hydroxyl groups per α–CD, each of them could bind with numerous neighboring α-CDs. However, Figure 4a showed that the variation of the total dissolution enthalpy with N was dominated by the content of naked PEO units. All these results showed the relative contribution of each domain of PRs (*i.e.* the rotaxane blocks and the naked polymer segments of the PR) on the cohesion of the physical gels.

For all N, the total dissolution enthalpies were normalized by their values at the equilibrium state (*i.e.* when the gels were formed, at least 24 h) and plotted *versus* the aging time t_a (Figure 5a). At low t_a, the normalized dissolution enthalpy remained low before suddenly increasing with t_a till reaching a plateau value. We defined the

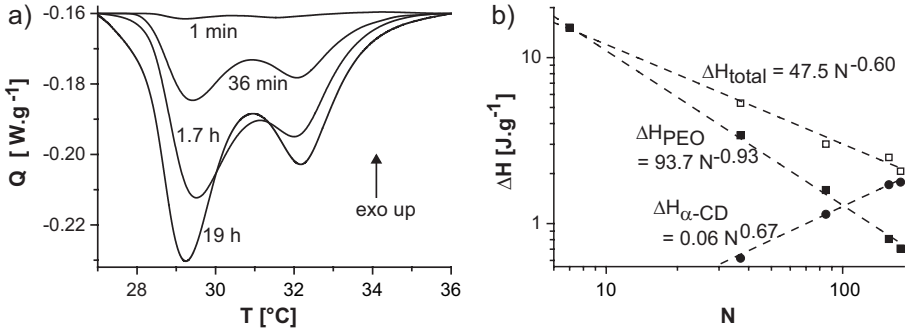

Figure 4.
DSC: a) Heat flow Q *versus* temperature T for PR_{85} at 19.6 w/w% in DMSO after different aging times (1 min, 36 min, 1.7 h and 19 h) at 21 °C. The heat flows are given in W g^{-1} of PR *solution*. b) (□) Total dissolution enthalpy ΔH_{total} calculated from the experimental curve, (■) naked PEO segment dissolution enthalpy ΔH_{PEO} obtained after deconvolution and (•) α-CD dissolution enthalpy $\Delta H_{\alpha-CD}$ obtained after deconvolution after a long aging time (typically 24 h) *versus* complexation degree N for PR solutions at 19.6 w/w% in DMSO.

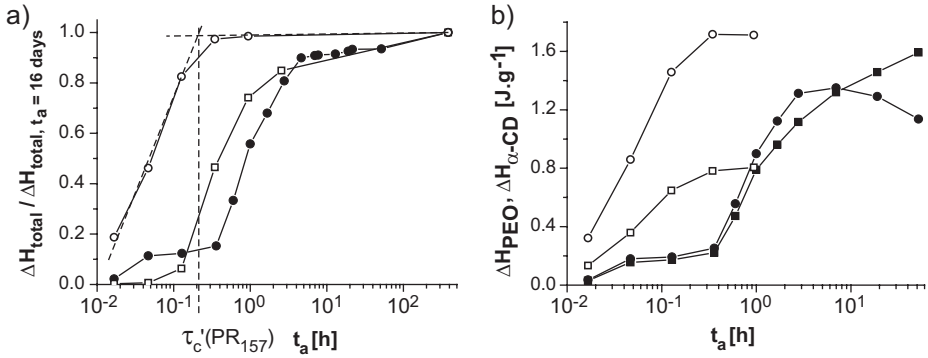

Figure 5.

DSC: a) Normalized total dissolution enthalpy ΔH_{total} *versus* aging time t_a at 21 °C for PRs at 19.6 w/w% in DMSO: (□) PR_7, (●) PR_{85} and (○) PR_{157}. The geometric construction leading to the estimation of the characteristic time τ_c' in the case of PR_{157} is shown on the graphic. b) (■) Naked PEO segment dissolution enthalpy ΔH_{PEO} in the case of PR_{85}, (●) α-CD dissolution enthalpy $\Delta H_{\alpha\text{-CD}}$ in the case of PR_{85}, (□) naked PEO segment dissolution enthalpy ΔH_{PEO} in the case of PR_{157} and (○) α-CD dissolution enthalpy $\Delta H_{\alpha\text{-CD}}$ in the case of PR_{157} obtained after deconvolution *versus* aging time t_a at 21 °C for PRs at 19.6 w/w% in DMSO. The absolute values of the dissolution enthalpies are presented here. They are given in J g^{-1} of PR *solution*.

characteristic time τ_c' as the intersection point between the tangent at the inflection point and the asymptote at long times. The resulting characteristic times depended on the complexation degree in a non-monotonous way as the characteristic times of gelation determined by RDA measurements (Figure 1b). The fastest kinetics was obtained for the lowest and the highest complexation degree values, when one contribution was predominant over the other one, whereas the intermediate complexation degree led to a slower gelation. For high N, the absolute values of the time obtained by DSC differed strongly from that obtained by RDA since these characterization methods exhibited different sensitivities to the generating structures.

The quantitative estimation of the α-CD contribution to the total dissolution enthalpy can now be discussed. For instance, a PR_{37} solution at 19.6 w/w% in DMSO exhibited a dissolution enthalpy after 52 h at 21 °C equal to 4.5 J g^{-1} of PR *solution*. Making the hypothesis that only α-CD hydroxyl groups were involved in the gelation process and thus contributed to the dissolution enthalpy, and taking a hydrogen bond dissociation enthalpy of 1780 J mol^{-1} of hydroxyl group,[22–24] it led to a percentage of hydroxyl groups participated in hydrogen bonding equal to 112%. This result suggested that all eighteen hydroxyl groups of every α-CD participated in the association which was not realistic for steric reasons. This confirmed that another contribution to gelation, originating from the local precipitation of PEO units, had to be taken into account. Moreover, $\Delta H_{\alpha\text{-CD}}$ and ΔH_{PEO}, obtained after deconvolution of the mass heat flows, were plotted as a function of the aging time t_a (Figure 5b). As soon as the gelation began, the ratio of ΔH_{PEO} over $\Delta H_{\alpha\text{–CD}}$ was constant up to 3 h. Thus, the generation of the naked PEO segment crystallites and this of the α-CD aggregates were simultaneous: Locally, the generation of one type of domain was induced by the other one.

Conclusion

PRs based on α-CDs threaded onto 22 kg mol^{-1} PEO chains in concentrated solution in DMSO formed physical gels when let at rest at temperatures below 25 °C. A wide range of complexation degrees, from $N = 7$ to $N = 176$ α-CDs threaded per PEO chain, was studied,

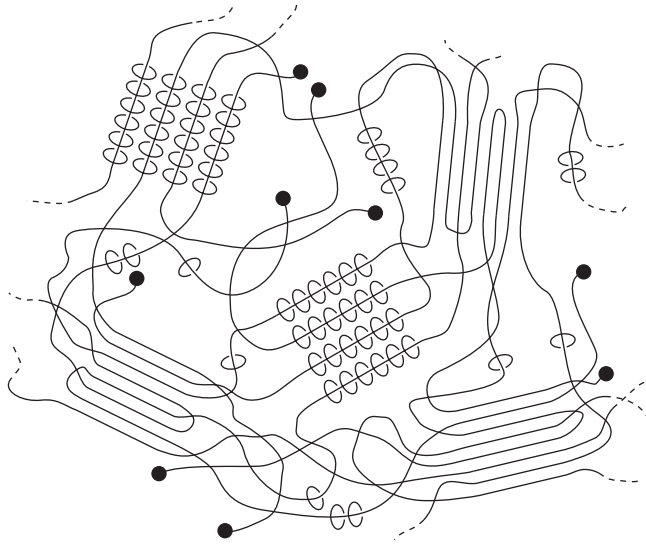

Figure 6.
Schematic view of the PR physical gel showing the two kinds of cross-linked domains: the crystal of naked PEO segments and the well-organized α-CD aggregates more or less swollen in DMSO. The physical cross-linked domains are separated by amorphous domains made of non-aggregated rotaxane or naked PEO blocks immersed in DMSO.

allowing the unambiguous identification of the origins of gelation (Figure 6). In particular, the cohesion of these physical gels was found to be due to two phenomena. First, it was due to the crystallization of naked PEO segments (the parts of the PR molecule not covered by α-CDs); indeed, naked PEO segments were in bad solvent conditions in DMSO at room temperature and thus formed crystal-like structures which dissolved at 29.4 °C. Second, the cohesion of these physical gels was also due to the aggregation of α-CDs through their hydroxyl groups in an intra- and intermolecular way; these well-organized structures dissolved at 32.0 °C.

The elastic modulus of the formed gels showed a non-monotonous dependence on *N*. Indeed, the elastic modulus was related to the concentration of physically cross-linked domains whose evolution with *N* had two distinct origins: The concentration of naked PEO segments forming crystals was high at low *N*, whereas the concentration of aggregated α-CD domains was higher at high *N*. Furthermore, the increase of the elastic modulus at high *N* was due to the increase of the PR stiffness and, consequently, to the stiffness of the strands between the physically cross-linked domains. Furthermore, the gelation kinetics was followed by mechanical and calorimetric experiments. Both techniques showed the same trend of the characteristic time *versus* *N*. The characteristic times exhibited a non-monotonous evolution with *N*. The fastest characteristic times were reached in the case of PRs with low complexation degree values due to their high flexibility and also in the case of PRs with high complexation degree values due to the presence of numerous α–CDs per PEO chain. At intermediate complexation degree values, the kinetics was much slower. The characteristic times determined through RDA were longer than those obtained by DSC. Indeed, RDA measurements probed the elasticity of the gel and were, therefore, only slightly sensitive to the first stages of the aggregation, before percolation was reached. In contrast, DSC measurements were sensitive to all types of aggregation events, whatever their size or structure, and thus led to the fastest kinetics.

With this study we showed that, even though DMSO can be considered as one of the best solvents for PRs based on PEO and α-CDs, physical gels formed at room temperature. The cohesion of these gels was due, on the one hand, to the crystallization of naked PEO segments of the PRs and, on the other hand, to the formation of well-organized α-CD aggregates driven by the intra- and inter-molecular hydrogen bonding interactions of their hydroxyl groups. Thus, in order to observe the dynamic behavior of the PRs due to the free sliding of α-CDs along the guest polymer chain, one needs to use PR/DMSO solutions at temperatures higher than 40 °C.

Acknowledgements: The authors are grateful to the grant "ANR Jeunes Chercheurs 2005 SUPRAGEL" (JC05_50625), to the CNRS, and to the Région Alsace (France) for financial support of this work.

[1] G. Wenz, B.-H. Han, A. Müller, *Chem. Rev.* **2006**, *106*, 782–817.
[2] G. Fleury, C. Brochon, G. Schlatter, G. Bonnet, A. Lapp, G. Hadziioannou, *Soft Matter* **2005**, *1*, 378–385.
[3] N. Jarroux, P. Guégan, H. Cheradame, L. Auvray, *J. Phys. Chem. B* **2005**, *109*, 23816–23822.
[4] M. Mutter, *Tetrahedron Lett.* **1978**, *19*, 2839–2842.
[5] Y. Fang, R. Takahashi, K. Nishinari, *Biomacromolecules* **2004**, *5*, 126–136.
[6] M. Takahashi, K. Yokoyama, T. Masuda, T. Takigawa, *J. Chem. Phys.* **1994**, *101*, 798–804.
[7] M. Williams, T. Foster, D. Martin, I. Norton, M. Yoshimura, K. Nishinari, *Biomacromolecules* **2000**, *1*, 440–450.
[8] A. Semenov, M. Rubinstein, *Macromolecules* **1998**, *31*, 1373–1385.
[9] F. Tanaka, W. Stockmayer, *Macromolecules* **1994**, *27*, 3943–3954.
[10] M. Gordon, S. Ross-Murphy, *Pure Appl. Chem.* **1975**, *43*, 1–26.
[11] K. Nishinari, *Colloid Polym. Sci.* **1997**, *275*, 1093–1107.
[12] M. Yoshimura, K. Nishinari, *Food Hydrocoll.* **1999**, *13*, 227–233.
[13] E. Pezron, A. Ricard, L. Leibler, *J. Polym. Sci., Part B: Polym. Phys.* **1990**, *28*, 2445–2461.
[14] R. Schultz, R. Myers, *Macromolecules* **1969**, *2*, 281–285.
[15] C. Özdemir, A. Güner, *Eur. Polym. J.* **2007**, *43*, 3068–3093.
[16] G. Fleury, G. Schlatter, C. Brochon, G. Hadziioannou, *Polymer* **2005**, *46*, 8494–8501.
[17] Y. Takahashi, H. Tadokoro, *Macromolecules* **1973**, *6*, 672–675.
[18] H. Klug, L. Alexander, in: "*X-Ray Diffraction Procedures for Polycrystalline and Amorphous Materials*", Wiley, New York (USA) 1974.
[19] I. Topchieva, A. Tonelli, I. Panova, E. Matuchina, F. Kalashnikov, V. Gerasimov, C. Rusa, M. Rusa, M. Hunt, *Langmuir* **2004**, *20*, 9036–9043.
[20] T. Girardeau, T. Zhao, J. Leisen, H. Beckham, D. Bucknall, *Macromolecules* **2005**, *38*, 2261–2270.
[21] A. Tonelli, *Macromolecules* **2008**, *41*, 4058–4060.
[22] J. Szejtli, in: "*Cyclodextrins and their Inclusion Complexes*", Akadémiai Kiadó, Budapest (Hungary) 1982.
[23] R. Gelb, L. Schwartz, J. Bradshaw, D. Laufer, *Bioorg. Chem.* **1980**, *9*, 299–304.
[24] R. Gelb, L. Schwartz, D. Laufer, *Bioorg. Chem.* **1982**, *11*, 274–280.

